This is a repository copy of *Electron transport and terahertz gain in quantum-dot cascades*
.

Electron Transport and Terahertz Gain in Quantum-Dot Cascades

Nenad Vukmirović, *Student Member, IEEE*, Dragan Indjin, Zoran Ikonić, and Paul Harrison, *Senior Member, IEEE*

Abstract—**Electron transport through quantum-dot (QD) cascades was investigated using the formalism of nonequilibrium Green's functions within the self-consistent Born approximation. Polar coupling to optical phonons, deformation potential coupling to acoustic phonons, as well as anharmonic decay of longitudinal optical phonons were included in the simulation. A QD cascade laser structure comprising two QDs per period was designed and its characteristics were simulated. Significant values of population inversion enabling lasing in the terahertz frequency range were predicted, with operating current densities being more than an order of magnitude smaller than in existing terahertz quantum-well-based quantum-cascade lasers.**

Index Terms—Electron transport, quantum-cascade lasers (QCLs), quantum dots (QDs), terahertz.

I. INTRODUCTION

IN RECENT years, there has been significant experimental and theoretical interest in the possibility of the development of intraband lasers based on quantum dots (QDs) [1]–[5]. Due to the truly discrete electronic spectra of QDs, most of the undesired scattering and relaxation processes are suppressed, and such devices are expected to have two orders of magnitude lower threshold currents than the corresponding quantum-well-based devices. Experimental evidence that the system with truly discrete states should have a lower threshold current comes from extremely low threshold currents observed in quantum-well-based quantum-cascade lasers (QCLs) in strong magnetic fields [6]. Electroluminescence from combined QD–quantum-well superlattice structures has been observed by several groups [1]–[3], [7]. After the initial theoretical proposals of QD intraband lasers [8], [9], only a few theoretical studies of this type of device were reported [5], [10]. However, a detailed transport model through such structures has not yet been developed. In this work, a nonequilibrium Green's functions (NGF) theory [11] of steady-state transport through periodic arrays of multiple QDs is applied to design and evaluate the output characteristics of a QD cascade structure.

II. THEORETICAL FRAMEWORK

The electronic miniband structure of a QD superlattice is solved using the eight-band strain-dependent $\boldsymbol{k} \cdot \boldsymbol{p}$ method [12]. The delocalized superlattice states obtained that way were then used to construct well localized states. These were subsequently used for steady-state transport calculation using

the NGF formalism. The regime of relatively low carrier and doping densities is investigated, where the interaction with impurities and carrier–carrier interaction can be neglected, as well as when formation of electric field domains does not occur. In this region, the current depends linearly on the carrier density; therefore, it has been divided by the total occupancy of states in one period of the structure, in the field–current characteristics presented. The interaction of electrons with polar longitudinal optical (LO) phonons described via the Frölich Hamiltonian, and the deformation potential interaction with longitudinal acoustic phonons are considered. Bulk phonon modes are assumed as several studies of intraband quantum-well lasers in the absence [13] and presence [14] of magnetic field show that this approach is quite satisfactory. The effect of strain on phonon modes was not considered either, as the corresponding strain-induced shifts [15] are of the order of 1 meV. Self-energies due to these interactions are both modeled within the self-consistent Born approximation. The anharmonic decay of LO phonons, which is known to be important for a proper description of the relaxation processes in QDs, is also taken into account by adding a finite linewidth (corresponding to the lifetime of 5 ps, which is within the range of lifetimes reported in [16]) to the Green's functions of free phonons. A system of algebraic equations (for the retarded Green's functions $G_{\alpha\beta}^{R}(E)$, the lesser Green's functions $G_{\alpha\beta}^{<}(E)$, and the self-energies $\Sigma_{\alpha\beta}^{R}(E)$ and $\Sigma_{\alpha\beta}^{<}(E)$) containing the Dyson equation, the Keldysh relation, and the expressions for self-energies [11], [17] is then solved self-consistently. The current through the structure is calculated as in [18] and involves only contributions from the off-diagonal lesser Green's functions (i.e., from coherences between states rather than populations of states). More technical details of the theoretical framework are presented in [19].

III. RESULTS

From a purely theoretical point of view, QDs provide additional degrees of freedom in design in comparison to quantum wells, as both the dimensions in the growth and lateral directions can be varied in principle. However, controllability of the dot dimensions is not that mature, and a realistic design should involve as few QDs per period as possible. A design comprising two QDs per period is presented here. The scheme of the design principle for the structure is shown in Fig. 1. One period of the structure consists of two dots A and B of different sizes. The state originating mainly from dot A is designed to be the upper laser level and the state originating from dot B is the lower laser level. In order to get population inversion in the structure, the depopulation rate of the lower laser level (transition $B_2 \rightarrow A_1$ in Fig. 1) should be faster than its population rate (transition $A_2 \rightarrow B_2$ in Fig. 1). This is achieved by engineering the energy of the $B_2 \rightarrow A_1$ transition to be close to one LO phonon
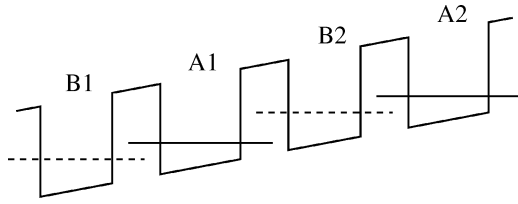
Fig. 1. Energy levels scheme of a QD cascade structure. Two periods of the structure are presented.
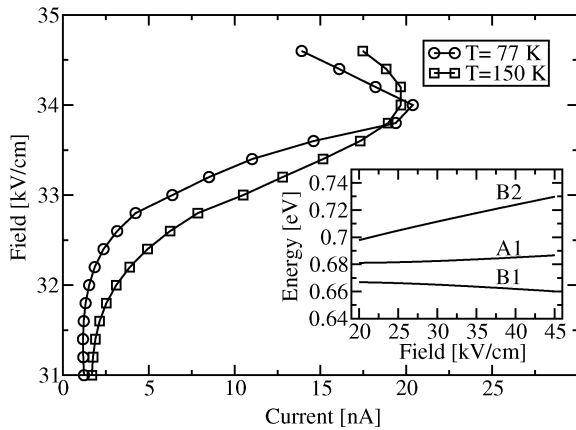

Fig. 2. Field-current characteristics of the prototype of a QD cascade laser structure at temperatures $T = 77$ K and $T = 150$ K. Inset: dependence of energy levels on electric field.
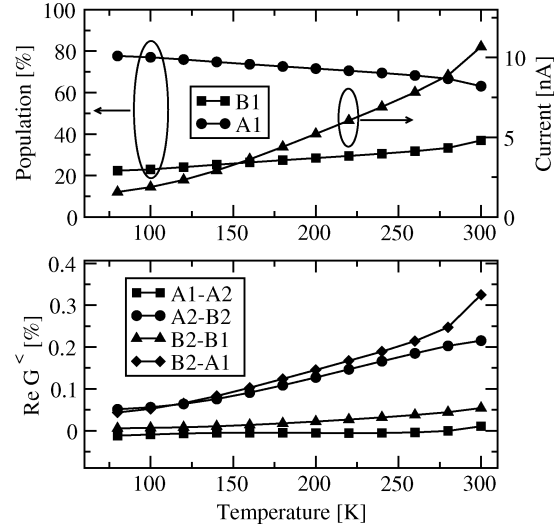

Fig. 3. Temperature dependence of populations of energy levels (top panel, left axis), current (top panel, right axis), and real part of coherences among states (bottom panel) at the field $F = 32$ kV/cm.

energy, while the lasing transition $(A_2 \rightarrow B_2)$ energy is significantly smaller than that. This makes the populations of energy levels in the design robust to QD nonuniformities, as large energy level fluctuations are required to break this order of energy levels. The nonuniformities then mainly affect the gain through the increased transition linewidth, as will be discussed later. The barrier between the dots is thin enough to provide significant electronic coupling between the dots. This provides wavefunction overlap sufficient both for large values of the optical matrix element on the lasing transition and a large transition rate on the lower laser level depopulation transition.

The above conditions are fulfilled when the dot dimensions are chosen as follows. Lens-shaped InAs–GaAs QDs are assumed, with the dot diameters set to $D = 20$ nm. The height of dot A is set to $h_A = 5$ nm and the height of dot B to $h_B = 4.5$ nm. All barriers between the dots are set to 3 nm. The field-current characteristics of the structure at temperatures $T = 77$ K and $T = 150$ K around the design field are presented in Fig. 2. Two levels per period originating from ground states of dots A and B were included in the simulation. Excited states of dots A and B, being ∼70 meV above the ground state, are weakly populated at these temperatures and do not contribute to the electron transport.

The region of negative differential resistivity occurs at the field of $F = 34$ kV/cm when the $B_2 \rightarrow A_1$ transition energy becomes equal to one LO phonon energy. In this structure, population inversion between B_2 and A_2 is present in the whole range of fields investigated in Fig. 2, not only around the peak in the characteristics. This is a consequence of the fact that in this range the separation between levels B_2 and A_1 is still considerably larger than between A_1 and B_1 (see inset in Fig. 2).

As low current is desirable for device operation in order to reduce heat dissipation, the field of $F = 32$ kV/cm is adopted as the design field for the structure. It is also important to note that the current–field characteristic exhibits positive differential resistivity in this region and, therefore, stable operation of the device should be feasible. The design also allows a certain degree of electric field tunability, as for example in the range of fields from 31 to 34 kV/cm, the transition energy changes by 10% (see inset in Fig. 2).

Temperature dependence of populations, current, and coherences among states at the design field is shown in Fig. 3. From coherences presented, one can verify that the electron transport path is in accordance with the designed path. Real parts of the coherences among pairs of states $B_2 - A_1$ and $A_2 - B_2$ are much larger than the same quantities among other pairs of states (see Fig. 3), implying that electron transport does take place via a sequence of transitions $A_2 \rightarrow B_2 \rightarrow A_1 \rightarrow B_1 \rightarrow, \dots$, as desired. Nonzero values of coherences $A_1 - A_2$ and $B_2 - B_1$ imply that there is a certain degree of current leakage from the designed transport path. While this undesired transport path is weakly present at the design field, it does become important at lower fields. Consequently, another peak in the current-field characteristics arises at $F \approx 23$ kV/cm when the potential drop per period is equal to one LO phonon energy. This is the region of fields which should be avoided for QCL device operation. The presence of this current peak, being larger than the peak in the designed operating region, is likely to prevent one to bring the structure to the region of stable device operation by current pumping. A different approach is, therefore, necessary, and we believe that this can be achieved by continuous sweep-up of the bias towards the designed bias value. Alternatively, or in combination with voltage sweep-up, one can use a bypass resistive structure [20] for improved bias field stabilization.

Next, the value of the gain in the structure is estimated from the calculated populations of the energy levels. The gain should in principle be calculated from the self-consistent procedure as described, for example, in [17]. Here, an estimate will be given
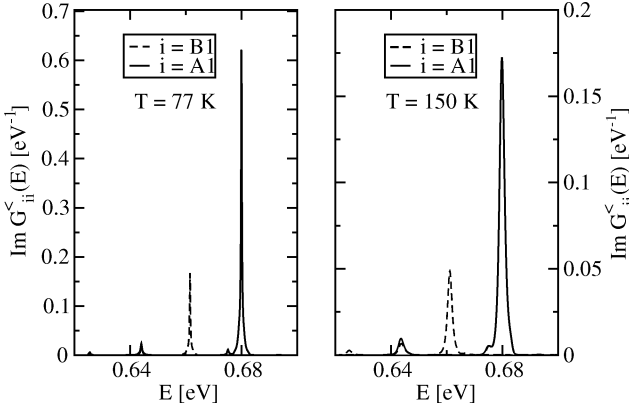
Fig. 4. Energy distribution of the population of the upper (full line) and lower (dashed line) laser level of the prototype of a QD cascade laser structure at the field $F = 32$ kV/cm and temperatures of $T = 77$ K (left) and $T = 150$ K (right).

based on a semiclassical expression given in [4], that also phenomenologically takes into account broadening due to inhomogeneities of the QD ensemble by assuming a Gaussian lineshape on the transition. The standard deviation of the Gaussian function is then a measure of the nonuniformities of the QD ensemble. A full-width at half-maximum equal to 12% of the transition energy is assumed, a value larger than the linewidths of the imaginary part of the lesser Green's functions $G_{\alpha\alpha}^{<}(E)$ (representing the energy distribution of the population of level α), presented in Fig. 4 for the field of $F = 32$ kV/cm. This approach would, therefore, underestimate the value of the gain for highly uniform samples. The calculated population inversion between the upper and lower laser level at the design field is 56% at $T = 77$ K and decreases with temperature (Fig. 3). It should be mentioned that at higher temperatures approaching room temperature, population inversion is most likely smaller than the value predicted here from the simulation involving ground states of QDs only, as a certain number of carriers is present in the QD excited states as well. The transition energy is equal to 19 meV corresponding to a frequency of 4.6 THz. The calculated value of the optical cross section for z-polarized radiation on the transition is $\sigma \approx 1.5 \times 10^{-13}$ cm^2. Assuming the carrier density of 10^{10} cm^{-2} and a population inversion of $\sim 50\%$, one obtains a gain of $g \approx 470$ cm^{-1}, which is sufficient for lasing since typical waveguide losses in terahertz QCLs are much smaller. The operating current density at the design field is then equal to $J \approx 15$ A/cm^2, opposed to terahertz quantum-well-based QCLs [21], where the threshold current density is more than an order of magnitude larger.

In conclusion, transport through QD cascade structures was investigated using the formalism of NGF. A suitable structure for exhibiting population inversion and consequently the gain at terahertz frequencies in the region of positive differential resistivity was identified. Superior performance in comparison to quantum-well-based QCLs was predicted.

ACKNOWLEDGMENT

REFERENCES

[1] S. Anders, L. Rebohle, F. F. Schrey, W. Schrenk, K. Unterrainer, and G. Strasser, "Electroluminescence of a quantum dot cascade structure," *Appl. Phys. Lett.*, vol. 82, no. 22, pp. 3862–3864, 2003.

[2] N. Ulbrich, J. Bauer, G. Scarpa, R. Boy, D. Schuh, G. Abstreiter, S. Schmult, and W. Wegscheider, "Midinfrared intraband electroluminescence from AlInAs quantum dots," *Appl. Phys. Lett.*, vol. 83, no. 8, pp. 1530–1532, 2003.

[3] C. H. Fischer, P. Bhattacharya, and P. C. Yu, "Intersublevel electroluminescence from $In_{0.4}Ga_{0.6}As$/GaAs quantum dots in quantum cascade heterostructure with GaAsN/GaAs superlattice," *Electron. Lett.*, vol. 39, no. 21, pp. 1537–1538, Oct. 2003.

[4] N. Vukmirović, Z. Ikonić, V. D. Jovanović, D. Indjin, and P. Harrison, "Optically pumped intersublevel midinfrared lasers based on InAs–GaAs quantum dots," *IEEE J. Quantum Electron.*, vol. 41, no. 11, pp. 1361–1368, Nov. 2005.

[5] I. A. Dmitriev and R. A. Suris, "Quantum cascade lasers based on quantum dot superlattice," *Phys. Stat. Sol.*, vol. 202, pp. 987–991, 2005.

[6] G. Scalari, S. Blaser, J. Faist, H. Beere, E. Linfield, D. Ritchie, and G. Davies, "Terahertz emission from quantum cascade lasers in the quantum hall regime: Evidence for many body resonances and localization effects," *Phys. Rev. Lett.*, vol. 93, no. 23, p. 237403, Dec. 2004.

[7] D. Wasserman, C. Gmachl, S. A. Lyon, and E. A. Shaner, "Multiple wavelength anisotropically polarized mid-infrared emission from InAs quantum dots," *Appl. Phys. Lett.*, vol. 88, p. 191118, 2006.

[8] N. S. Wingreen and C. A. Stafford, "Quantum-dot cascade laser: Proposal for an ultralow-threshold semiconductor laser," *IEEE J. Quantum Electron.*, vol. 33, no. 7, pp. 1170–1173, Jul. 1997.

[9] C.-F. Hsu, J.-S. O. P. Zory, and D. Botez, "Intersubband quantum-box semiconductor lasers," *IEEE J. Sel. Topics Quantum Electron.*, vol. 6, no. 3, pp. 491–503, May 2000.

[10] V. M. Apalkov and T. Chakraborty, "Luminescence spectra of a quantum-dot cascade laser," *Appl. Phys. Lett.*, vol. 78, no. 13, pp. 1820–1822, Mar. 26, 2001.

[11] H. Haug and A.-P. Jauho, *Quantum Kinetics in Transport and Optics of Semiconductors*. Berlin: Springer, 1996.

[12] N. Vukmirović, Ž. Gačević, Z. Ikonić, D. Indjin, P. Harrison, and V. Milanović, "Intraband absorption in InAs/GaAs quantum dot infrared photodetectors—Effective mass versus $k \cdot p$ modelling," *Semicond. Sci. Technol.*, vol. 21, pp. 1098–1104, 2006.

[13] P. Kinsler, P. Harrison, and R. W. Kelsall, "Intersubband terahertz lasers using four-level asymmetric quantum wells," *J. Appl. Phys.*, vol. 85, no. 1, pp. 23–28, Jan. 1, 1999.

[14] M. Erić, V. Milanović, Z. Ikonić, and D. Indjin, "Simulation of optically pumped intersubband laser in magnetic field," *Solid State Commun.*, vol. 142, pp. 605–609, 2007.

[15] J. Ibanez, A. Patane, M. Henini, L. Eaves, S. Hernandez, R. Cusco, L. Artus, Y. G. Musikhin, and P. N. Brounkov, "Strain relaxation in stacked InAs/GaAs quantum dots studied by Raman scattering," *Appl. Phys. Lett.*, vol. 83, no. 15, pp. 3069–3071, 2003.

[16] A. R. Bhat, K. W. Kim, and M. A. Stroscio, "Theoretical calculation of longitudinal-optical-phonon lifetime in GaAs," *J. Appl. Phys.*, vol. 76, no. 6, pp. 3905–3907, Sep. 15, 1994.

[17] S.-C. Lee and A. Wacker, "Nonequilibrium Green's function theory for transport and gain properties of quantum cascade structures," *Phys. Rev. B*, vol. 66, p. 245314, 2002.

[18] S.-C. Lee, F. Banit, M. Woerner, and A. Wacker, "Quantum mechanical wavepacket transport in quantum cascade laser structures," *Phys. Rev. B*, vol. 73, p. 245320, 2006.

[19] N. Vukmirović, Z. Ikonić, D. Indjin, and P. Harrison, "Quantum transport in semiconductor quantum dot superlattices: Electron-phonon resonances and polaron effects," *Phys. Rev. B*, vol. 76, no. 24, p. 245313, 2007.

[20] E. S. Daniel, B. K. Gilbert, J. S. Scott, and S. J. Allen, "Simulations of electric field domain suppression in a superlattice oscillator device using a distributed circuit model," *IEEE Trans. Electron Devices*, vol. 50, no. 12, pp. 2434–2444, Dec. 2003.

[21] S. Kumar, B. S. Williams, Q. Hu, and J. L. Reno, "1.9 THz quantum-cascade lasers with one-well injector," *Appl. Phys. Lett.*, vol. 88, p. 121123, 2006.